A Novel Anticancer Effect of Thalidomide: Inhibition of Intercellular Adhesion Molecule-1–Mediated Cell Invasion and Metastasis through Suppression of Nuclear Factor-κB

Yi-Chu Lin,[1] Chia-Tung Shun,[2] Ming-Shiang Wu,[3] and Ching-Chow Chen[1]

Abstract

Purpose: Thalidomide has been reported to have antiangiogenic and antimetastatic effects. Intercellular adhesion molecule-1 (ICAM-1) was shown to be involved in monocyte adherence to epithelial cells and cancer cell invasion. In this study, we further investigated the role of ICAM-1 in tumorigenesis, including tumor formation and metastasis. ICAM-1 as a molecular target for cancer and the anticancer effect of thalidomide were investigated.

Experimental Design: Expression of ICAM-1 protein in human lung cancer specimens was assessed by immunohistochemistry. ICAM-1 overexpressing A549 cells (A549/ICAM-1) were established to investigate the direct effect of ICAM-1 on *in vitro* cell invasion and *in vivo* tumor metastasis. Transient transfection and luciferase assay, electrophoretic mobility shift assay, and chromatin immunoprecipitation were done to assess the activity and binding of nuclear factor-κB to the ICAM-1 promoter. A xenograft model in nude mice was conducted to evaluate the anticancer effect of thalidomide.

Results: High expression of ICAM-1 in human lung cancer specimens was correlated with a greater risk of advanced cancers (stages III and IV). A549/ICAM-1 cells were shown to induce *in vitro* cell invasion and *in vivo* tumor metastasis. Anti-ICAM-1 antibody and thalidomide had inhibitory effect on these events. Thalidomide also suppressed tumor necrosis factor-α–induced ICAM-1 expression through inhibition of nuclear factor-κB binding to the ICAM-1 promoter. The *in vivo* xenograft model showed the effectiveness of thalidomide on tumor formation.

Conclusion: These studies provide a framework for targeting ICAM-1 as a biologically based therapy for cancer, and thalidomide might be effective in human lung cancer.

Lung cancer is the major cause of malignancy-related deaths worldwide. Its high mortality and poor prognosis are due to the difficulty of early diagnosis, and high potential to invade locally and metastasize to distant organ (1). Despite advances in surgery, chemotherapy, and radiotherapy, survival benefits remains poor (2). Recent studies are focused on the molecular events leading to lung cancer and the development of molecular-targeted therapies (3). Cell adhesion molecules belonging to the integrin, cadherin, and immunoglobulin superfamily have been implicated in tumor progression (4). Intercellular adhesion molecule-1 (ICAM-1, also called CD54), a member of the immunoglobulin supergene family, is an inducible surface glycoprotein that mediates adhesion-dependent cell-to-cell interactions (5, 6). The extracellular domain of ICAM-1 is essential for the transendothelial migration of leukocytes from the capillary bed into the tissue (7), and ICAM-1 may also facilitate movement (or retention) of cells through the extracellular matrix (8). Our previous study found that ICAM-1 plays an important role in lung cancer cell invasion (9). ICAM-1 antibody or antisense ICAM-1 cDNA had also been reported to rescue the invasiveness of breast cancer cells (10). Tumors with high expression of ICAM-1 were correlated with metastasis, poor prognosis, and shorter survival time (11). Therefore, ICAM-1 might play a critical role in tumorigenesis, and its disruption may prevent metastasis.

ICAM-1 is expressed constitutively at low levels on endothelial cells and some lymphocytes and monocytes. Stimulation with inflammatory cytokines, such as interleukin-1, tumor necrosis factor (TNF-α), and IFN-γ, or with lipopolysaccharide has been documented to increase ICAM-1 expression on multiple cell types (12–14). The promoter region of human *ICAM-1* gene has been shown to contain putative recognition sequences for a variety of transcription factors, including nuclear factor-κB (NF-κB), activator protein-1, activator protein-2, and the IFN-stimulated response (15). NF-κB family proteins are essential for enhanced ICAM-1 expression, and inhibition of NF-κB suppresses the expression of ICAM-1, resulting in the reduction of lung cancer cell invasion (9).

Authors' Affiliations: [1]Department of Pharmacology, College of Medicine, National Taiwan University; and [2]Department of Forensic Medicine and Pathology and [3]Division of Gastroenterology, Department of Internal Medicine, National Taiwan University Hospital, Taipei, Taiwan

Received 6/8/06; revised 8/14/06; accepted 9/12/06.

Grant support: National Science Council of Taiwan grant NSC 94-2320-B002-098.

The costs of publication of this article were defrayed in part by the payment of page charges. This article must therefore be hereby marked *advertisement* in accordance with 18 U.S.C. Section 1734 solely to indicate this fact.

Requests for reprints: Ching-Chow Chen, Department of Pharmacology, College of Medicine, National Taiwan University, No. 1, Jen-Ai Road, Section 1, Taipei 10018, Taiwan. Phone: 886-2-23123456, ext. 8321; Fax: 886-2-23947833; E-mail: ccchen@ha.mc.ntu.edu.tw.

doi:10.1158/1078-0432.CCR-06-1393

Thalidomide was originally used to treat morning sickness, but was banned in the 1960s due to serious congenital birth defects. Despite its history as human teratogen, thalidomide is emerging as a treatment for inflammatory disease and cancers because of its antiangiogenic and anti-inflammatory effects (16). Different stages of clinical trials have been conducted to treat malignant diseases, such as hematologic cancers and solid tumors, including renal cell carcinoma; ovarian, breast, and androgen-independent prostate cancer (17–19). Rational drug design of specific small-molecule inhibitors with better pharmacologic profiles leads to the identification of a specific molecular target for thalidomide (16). In this study, ICAM-1 was shown to be a molecular target for lung cancer. We investigated its role in lung cancer metastasis and the effect of thalidomide. High expression of ICAM-1 was detected in advanced human lung cancers (stages III and IV), and ICAM-1–overexpressing A549 cells induced *in vitro* cell invasion and *in vivo* tumor metastasis. Thalidomide showed anti-ICAM-1 and antitumor effects on the *in vivo* xenograft tumor model. Its molecular mechanism was shown to act through attenuation of NF-κB binding to the ICAM-1 promoter. These studies provide a framework for targeting ICAM-1–dependent metastasis as a biologically based therapy for cancer.

Materials and Methods

Materials. The plasmid encoding full-length human ICAM-1 cDNA was kindly donated by Dr. Geoffrey W. Krissansen (University of Auckland, Auckland, New Zealand). The ICAM-1 promoter construct, pIC1352, was a gift from Dr. P.T. van der Saag (Hubrecht Laboratory, Utrecht, the Netherlands). The NF-κB-luciferase expression plasmid was purchased from Stratagene (La Jolla, CA). Human TNF-α recombinant and mouse monoclonal anti-human ICAM-1 antibody were purchased from R&D Systems (Minneapolis, MN). The rabbit polyclonal antibodies specific for p65 and IKKα/β were purchased from Santa Cruz Biotechnology (Santa Cruz, CA). Anti-phospho-IKKα (Ser^{180})/β (Ser^{181}) and anti-phospho-p65 (Ser^{536}) antibodies were obtained from Cell Signaling (Danvers, MA). Reagents for SDS-PAGE were from Bio-Rad (Hercules, CA). [γ-^{32}P]ATP (3,000 Ci/mmol) was from Dupont-New England Nuclear (Beverly, MA). Thalidomide, a gift from TTY Biopharm (Taipei, Taiwan), was dissolved in DMSO.

Cell culture. A549 cells, an alveolar epithelial carcinoma cell line, were obtained from American Type Culture Collection (Manassas, VA), and cultured in DMEM supplemented with 10% fetal bovine serum, 100 units/mL penicillin, and 100 μg/mL streptomycin at 37°C in a humidified atmosphere of 5% CO_2/95% air.

Patients and specimens. Lung cancer specimens were obtained from a total of 40 patients who underwent surgical resection at the National Taiwan University Hospital from 2003 to 2005. Patients who had previous history of cancers or had been treated with neoadjuvant chemotherapy and radiation therapy were not included. Paraffin-embedded, formalin-fixed surgical specimens were collected for ICAM-1 immunohistochemical staining. Tumor size, local invasion, lymph node metastasis, and differentiation status were determined at pathologic examination. The final disease stage was determined by a combination of surgical and pathologic findings according to the current tumor-node-metastasis staging system for lung cancer. Follow-up data were obtained from the patients' medical charts and from our tumor registry service.

Immunohistochemistry. The 4-μm sections of paraffin-embedded tissue on glass slides were rehydrated and incubated in 3% hydrogen peroxide to block the endogenous peroxidase activity. After trypsinization, sections were blocked by incubation in 3% bovine serum albumin in PBS. The primary antibody monoclonal mouse anti-human ICAM-1 antibody (Novocastra, Newcastle, United Kingdom) was applied to the slides at a dilution of 1:25 (diluted in 3% bovine serum albumin) and incubated at 4°C overnight. After three washes in PBS, the samples were treated with goat anti-mouse IgG biotin-labeled secondary antibodies at a dilution of 1:50 (diluted in 0.05% PBS-Tween 20). Bound antibodies were detected with an ABC kit (Vector Laboratories). The slides were stained with chromogen diaminobenzidine, washed, counterstained with Delafield's hematoxylin, dehydrated, treated with xylene, and mounted. A score system from level 0 (no expression) to level 2 (highest expression) was established based on a positive staining area for ICAM-1 expression in tumors. Low and high ICAM-1 expression were defined by the levels 0, 1, and 2, respectively. Level 0 represents <5% of cells showing ICAM-1 expression, level 1 represents 6% to 50%, and level 2 represents 51% to 100%.

Stable transfected clone selection. Purified plasmid of human full-length ICAM-1 cDNA (3 μg) was transfected into A549 cells with TransFast transfection reagent. Twenty-four hours after transfection, stable transfectants were selected in gentamicin (G418; Invitrogen, Carlsbad, CA) at a concentration of 600 μg/mL. Thereafter, the selection medium was replaced every 3 days. After 2 weeks of selection in G418, clones of resistant cells were isolated and allowed to proliferate in medium containing G418 at 100 μg/mL.

Flow cytometry detection of ICAM-1 expression. ICAM-1 expression was determined by flow cytometry using an anti-ICAM-1 antibody and analyzed on a FACScalibur with Cellquest software.

Cell growth assays. A549/ICAM-1 cells were grown under 0.1% serum DMEM, and cell growth was measured using 3-(4,5-dimethylthiazol-2-yl)-2,5-diphenyltetrazolium bromide (Sigma, St. Louis, MO) colorimetric method.

In vitro *invasion assay.* The invasion assay was carried out using Transwell cell culture chambers (Corning Costar 3422, Corning, Cambridge, MA) as previously described (9). Briefly, polyvinylpyrrolidone-free polycarbonate filters (8.0-μm pore size, Nuclepore, Pleasanton, CA) were precoated with 5 μg Matrigel (BD Biosciences, Bedford, MA) on the upper surface. A549 cells were harvested with 1 mmol/L EDTA and then resuspended in DMEM supplemented with 0.1% fetal bovine serum. Cell suspensions (10^4 cells) were added to the upper compartment of the chamber. Cells were challenged with TNF following pretreatment with thalidomide for 30 minutes. After 24-hour incubation, the top side of the insert membrane was scrubbed free of cells with a cotton swab and the bottom side was fixed with 3.7% paraformaldehyde, stained with 0.5% crystal violet in 20% methanol. The crystal violet dye retained on the filters was extracted with DMSO and colorimetrically assessed by measuring its absorbance at 590 nm on an ELISA reader (Bio-Tek, Birmingham, United Kingdom).

In vivo *metastasis assay.* A549/Mock and A549/ICAM-1 cells were resuspended in PBS. Subsequently, 5×10^6 cells in 0.1 mL of PBS were injected into the lateral tail vein of 6-week-old nude mice. In anti-ICAM-1 antibody experiment, mice were randomly divided into two groups: The control group was i.v. injected with PBS, whereas the other group was i.v. injected with anti-ICAM-1 antibody (0.8 mg/g) on the 1st and 8th day. In thalidomide experiment, mice were randomly divided and orally received either vehicle (soy oil) or thalidomide (200 mg/kg/d) suspended in soy oil everyday. Mice were killed after 2 weeks, and all organs were examined for metastasis formation. The lungs were removed and fixed in 10% formalin. The number of lung tumor colonies was counted. Representative lung tumors were removed, fixed, and embedded in paraffin. Embedded tissue was sectioned into 4-μm sections, and the sections were stained with H&E for histologic analysis. All animal work was done under protocols approved by the Institutional Animal Care and Use Committee of the College of Medicine, National Taiwan University.

Quantification of ICAM-1 expression. The level of cell surface ICAM-1 expression was determined by ELISA as described previously (20).

Reverse transcription-PCR. Total RNA was isolated from A549 cell using Trizol reagent (Life Technologies). Two micrograms of total RNA were reverse transcribed into cDNA using oligo(dT) primer, then

amplified for 30 cycles using two oligonucleotide primers derived from published ICAM-1 or β-actin sequence, including 5′-TGCGGCTGCTAC-CACAGTGATGAT-3′ and 5′-CCATCTACAGCTTTCGGCGCCCA-3′ (ICAM-1), or 5′-TGACGGGGTCACCCACACTGTGCCCATCTA-3′ and 5′-CTAGAAGCATTTGCGGG GACGATGGAGGG-3′ (β-actin). The PCR products were subjected to 1.5% agarose gel electrophoresis.

Transient transfection. The vectors (pIC339, κB, and β-galactosidase reporters) were transiently transfected into A549 cells with Tfx-50 transfection reagent (Promega, Madison, WI). Briefly, 2 μg of plasmid DNA and 1 μg of β-gal and 3 μL transfection reagents were mixed, and the transfection protocol was carried out according to the manufacturer's instructions (Promega). Six hours after transfection, the cells were cultured in normal complete medium for another 16 hours. The transfected cells were subjected to luciferase assay.

Electrophoretic mobility shift assay. Oligonucleotides corresponding to the consensus sequences of NF-κB (5′-AGCTTGGAAATTCCGGA-3′) and of the human ICAM-1 promoter (5′-TTCCGGAATTTCCAAGCT-3′) were synthesized, annealed, and end labeled with [γ-^{32}P]ATP using T4 polynucleotide kinase. Electrophoretic mobility shift assay was done as previously described (20).

Chromatin immunoprecipitation assay. Chromatin immunoprecipitation assay analysis was done as described (21). Immunoprecipitated DNA was purified, resuspended in H_2O, and subjected to PCR. To amplify the regions of ICAM-1 promoter, PCR was done with the following pair of primers: 5′-AGACCTTAGCGCGGTGTAGA-3′ and 5′-GCGACTCGAGGAGACGATGA-3′. PCR products were then resolved by 1.5% agarose-ethidium bromide gel electrophoresis and visualized by UV.

Western blot analysis. Following treatment with thalidomide, total cell lysates or nuclear extracts were prepared and subjected to SDS-PAGE using 10% polyacrylamide gels as described previously (12).

Immunofluorescence staining. A549 cells, grown on coverslips, were pretreated with 1 μmol/L thalidomide for 30 minutes before incubation with 10 ng/mL TNF-α for 60 minutes. The immunofluorescence staining was done as previously described (12).

Animal xenograft assay. Four- to 6-week-old female BALB/c nude mice were injected with 10^7 A549 cells (suspended in 0.1 mL PBS and mixed with 0.1 mL Matrigel) in the rear left flank. Two weeks after administration, 100 to 200 mm^3 tumors were apparent on all mice. At this time, animals were divided into two groups (n = 6), and orally received either control vehicle (soy oil) or thalidomide (200 mg/kg/d) suspended in soy oil. Mice were treated everyday for 30 days with thalidomide or control vehicle, and tumor growth was measured twice per week with calipers. Tumor volume was calculated using the formula V (mm^3) = 0.52 × [ab^2], where a is the length and b is the width of the tumor.

Statistical analysis. All results were presented as mean ± SE. The two-tailed Student's t test was used to calculate the statistical significance between groups. Pearson χ^2 test was used to compare the clinicopathologic characteristics of patients with high ICAM-1 and low ICAM-1 expression. ANOVA test was used to compare the growth rate and tumor growth.

Results

Association of ICAM-1 protein expression with the status of patients having lung adenocarcinoma. Specimens from 40 patients with lung adenocarcinoma were analyzed by immunohistochemistry. Differential expression of ICAM-1 protein was detected in different cancer status. ICAM-1 was negative in normal lung epithelium, but was expressed in stage I (level 1), stage II (level 1), stage III (level 2), and stage IV (level 2) adenocarcinoma (Fig. 1A-E). ICAM-1 expression was predominately localized to the membrane (*black arrows*) and was also prominent (level 2) in squamous carcinoma (Fig. 1F).

Whether the level of ICAM-1 was related to prognostic factor for lung cancer was examined. As shown in Table 1, two groups of patients were divided according to the low (levels 0 and 1) or high expression of ICAM-1 (levels 2), respectively. The group with high expression was found to be associated with higher stage of disease, tumor status, lymph node metastasis, metastatic nodules, and poor differentiation. Thus, the expression of ICAM-1 was correlated with patients having lung metastasis.

Invasion and metastasis induced by A549/ICAM-1 alveolar epithelial cells and the inhibitory effect of thalidomide. Because ICAM-1 expression was associated with the tumor status in human lung cancer, ICAM-1 stable clone was established to further clarify the direct role of ICAM-1 in tumorigenesis. After

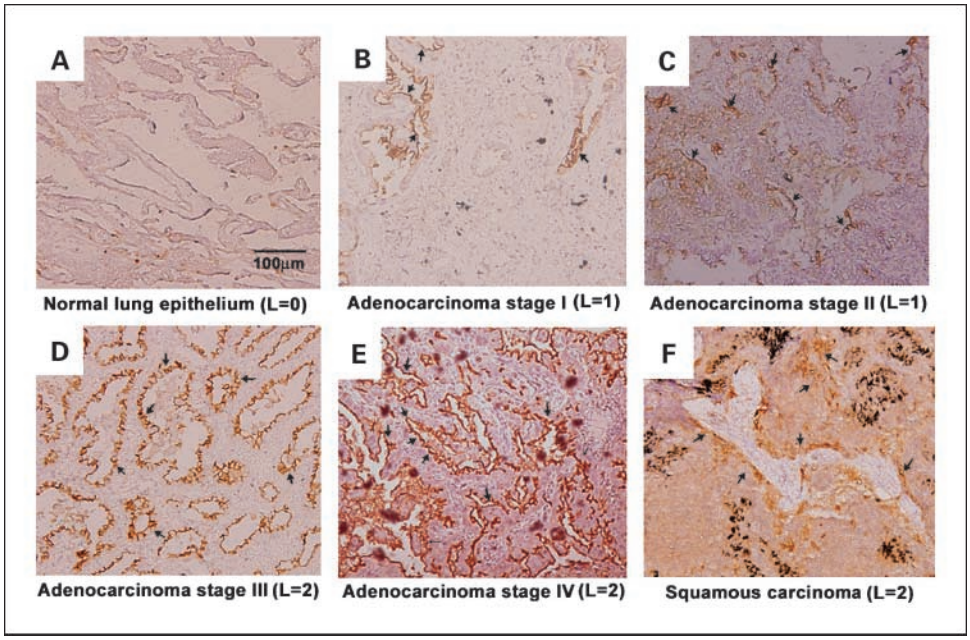

Fig. 1. Immunohistochemistry of ICAM-1 expression in human lung cancer specimens. *A,* representative staining of normal lung epithelium. Areas with normal epithelial cells are stained negative for ICAM-1 [level (*L*) 0]. *B,* representative section of stage I lung adenocarcinoma was stained positive for ICAM-1 (level 1). *C,* representative section of stage II lung adenocarcinoma (level 1). *D,* representative section of stage III lung adenocarcinoma (level 2). *E,* representative section of stage IV lung adenocarcinoma (level 2). *F,* representative section of lung squamous carcinoma at level 2 (*black arrows*).

Table 1. Clinicopathologic characteristics of tumors with high and low expression of ICAM-1 protein

Characteristic	Low ICAM-1 expression	High ICAM-1 expression	*P*
No.	20	20	
Age, y (mean ± SD)	63.5 ± 9.3	59.9 ± 10	0.25*
Sex, no. patients †			
Male	6	9	
Female	14	11	0.51
Stage, no. patients †			
I and II	16	7	
III and IV	4	13	0.01
Tumor status, no. patients †			
T_1 and T_2	16	11	
T_3 and T_4	4	9	0.18
Lymph nodal status, no. patients †			
N_0	16	8	
N_{1-3}	4	12	0.02
Metastatic nodal status, no. patients †			
M_0	20	16	
M_1	0	4	0.10
Differentiation, no. patients †			
PD	4	6	
MD	5	10	
WD	11	4	0.07

Abbreviations: PD, poorly differentiated; MD, moderately differentiated; WD, well differentiated.
**P* value for age was derived with a two-sided Student's *t* test; other *P* values were derived with a two-sided Pearson's χ^2 test.
†The stage, tumor status, lymph nodal status, and metastatic nodal status were classified according to the international staging system for lung cancer.

G418 selection, two ICAM-1–overexpressing A549 clones (A549/ICAM-1) and the corresponding vector control (A549/Mock) were isolated. Overexpression of ICAM-1 in A549/ICAM-1 cells was confirmed by Western blotting and fluorescence-activated cell sorting analysis (Fig. 2A). Its growth rate was greater than that of A549/Mock cells (Fig. 2B). The invasive capacity of A549/ICAM-1 cells across Matrigel was also greatly enhanced than that of A549/Mock, and this effect was attenuated by the anti-ICAM-1 antibody and by thalidomide in a dose-dependent manner (Fig. 2C and D).

The role of ICAM-1 in metastatic colonization was assessed by i.v. injection of A549/Mock and A549/ICAM-1 cells into the lateral tail vein of nude mice. Mice injected with A549/ICAM-1 had numerous large lung metastatic nodules, whereas those injected with A549/Mock cells had fewer and smaller nodules. I.v. injection with anti-ICAM-1 antibody or oral administration of thalidomide decreased the metastatic nodules (Fig. 2E and F).

Inhibitory effect of thalidomide on TNF-α–induced cell invasion and ICAM-1 expression. Previous study had found that ICAM-1 expression induced by TNF-α elicited cell invasion (9); therefore, the effect of thalidomide on TNF-α–induced ICAM-1–dependent cell invasion was also examined. As shown in Fig. 3A, thalidomide inhibited TNF-α–induced cell invasion in a dose-dependent manner. It also inhibited TNF-α–induced ICAM-1 protein and mRNA expressions (Fig. 3B and C). To elucidate the molecular mechanism, transient transfection was done using a human ICAM-1 promoter-luciferase construct, pIC339. Thalidomide inhibited TNF-α–induced ICAM-1 promoter activity in a dose-dependent manner (Fig. 3D).

Inhibitory effect of thalidomide on TNF-α–stimulated NF-κB activity and binding to the ICAM-1 promoter. Because NF-κB is critical for TNF-α–induced ICAM-1 expression (13), the effect of thalidomide on NF-κB activation was examined. The NF-κB luciferase activity and NF-κB–specific DNA-protein binding induced by TNF-α were inhibited by thalidomide in a dose-dependent manner (Fig. 4A and B). Chromatin immunoprecipitation assay showed that the *in vivo* binding of p65 to the ICAM-1 promoter was also inhibited by thalidomide (Fig. 4C).

Because TNF-α–stimulated NF-κB activity was inhibited by thalidomide, its effect on the IKK/IκBα/NF-κB pathway was further examined. When cells were treated with TNF-α for 5, 10, 30, or 60 minutes, phosphorylation of IKK was seen after a 5-minute treatment and was sustained for 10 minutes (Fig. 5A, *lanes 2-5*). These events were inhibited by thalidomide (Fig. 5A, *lanes 6-9*).

Phosphorylation of p65 transactivation domain at Ser^{536} was reported to increase the transcriptional activity of NF-κB. Therefore, Ser^{536} phosphorylation was examined using a specific anti-p65 phospho-Ser^{536} antibody. TNF-α–induced p65 phosphorylation was seen at a 5-minute treatment and was sustained for 60 minutes (Fig. 5A, *lanes 2-5*); this effect was also inhibited by thalidomide (Fig. 5A, *lanes 7-9*). The dose-response effect of thalidomide on the phosphorylation of IKK and p65 was further examined. As shown in Fig. 5B, TNF-α–induced IKK and p65 phosphorylations were both inhibited by thalidomide (Fig. 5B, *lanes 3-5*).

The translocation of NF-κB to the nucleus is tightly regulated by its interaction with the inhibitory IκBα; we further examined the nuclear translocation of p65 using Western blot and immunofluorescence. As shown in Fig. 5C, translocation of p65 to the nucleus was seen after treatment with TNF-α for 60 minutes (Fig. 5C, *lane 2*), but was not inhibited by 1 to 40 μmol/L thalidomide (Fig. 5C, *lanes 3-5*). Similar results were also shown by immunofluorescence (Fig. 5D).

Inhibitory effect of thalidomide on tumor growth of lung cancer xenograft and on metastasis. To further investigate the effect of thalidomide on the progression of lung cancer and metastasis, A549 cells were introduced into nude mice via s.c. administration. Fifteen days after injection, tumor formation of ~100 mm^3 was seen in all mice. Mice were then randomly selected for oral administration of thalidomide (200 mg/kg/d). As shown in Fig. 6A and B, a dramatic increase in tumor size and weight in nude mice on the 45th day after A549 cells injection was seen. The volume of tumor approached 2,000 mm^3 and the weight of tumor reached 1.85 g. After oral administration of thalidomide qd for 30 days, the tumor growth was inhibited by 63% and the tumor weight decreased to <1 g. No toxicity was found in mice treated with thalidomide.

Whether lung cancer xenograft model induced lung metastasis was also examined. After the 45th day of s.c. injection of A549 cells into nude mice, lung colonies were found. The metastatic lung nodules formed were measured to be 108.8; thalidomide treatment reduced this number to 67.3 (Fig. 6D). To further analyze the metastasis, histopathologic staining was done. Sections of lung stained with H&E showed the morphology of a typical lung adenocarcinoma, which disappeared after thalidomide treatment (Fig. 6C).

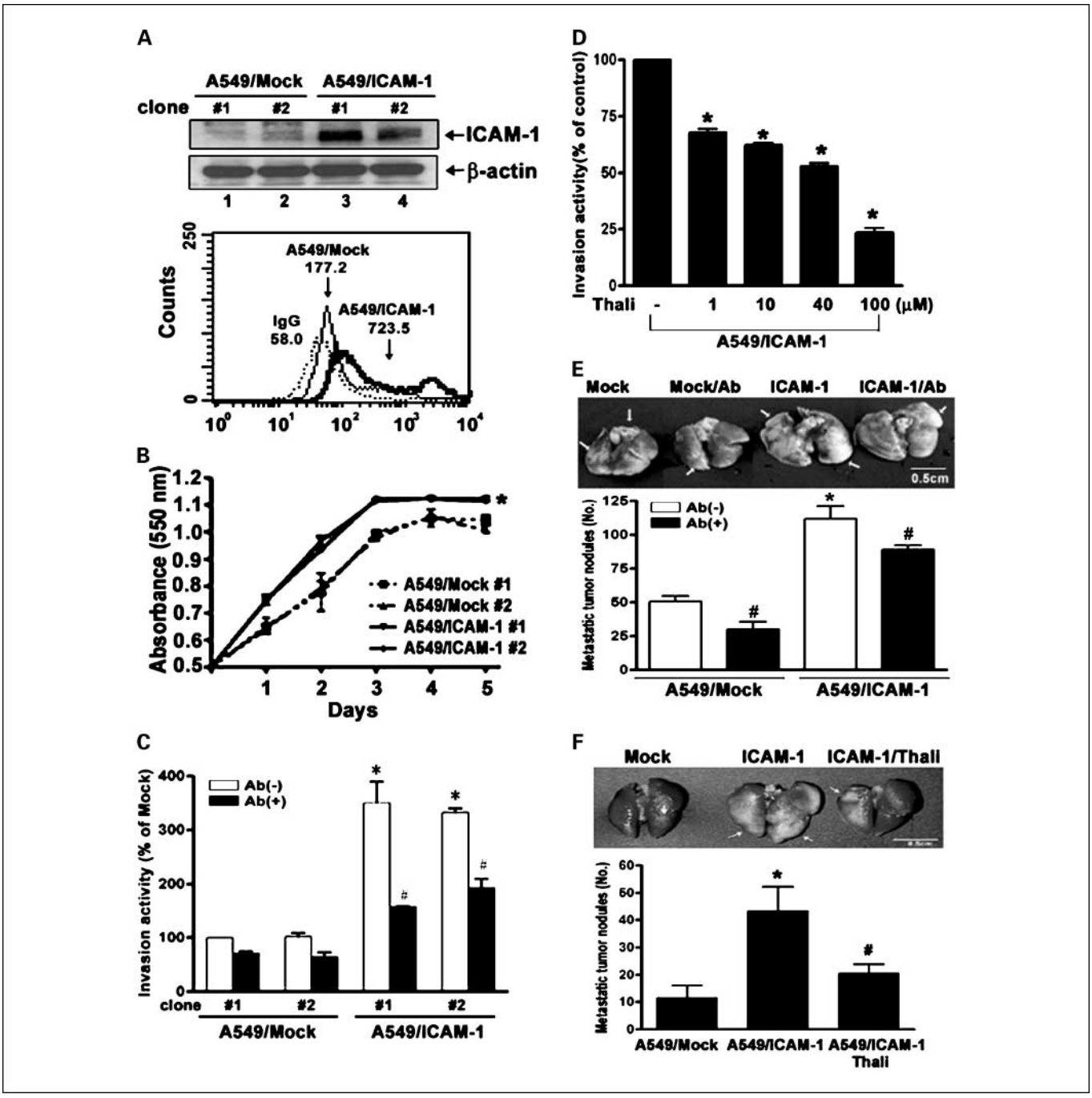

Fig. 2. ICAM-1 induces *in vitro* cell invasion, *in vivo* metastasis, and the inhibitory effect of thalidomide. *A,* top, Western blot analysis of the expression of ICAM-1 in two respective stable clones of A549/Mock and A549/ICAM-1 cells. Bottom, ICAM-1 expression was detected by fluorescence-activated cell sorting analysis. *B,* the growth rate was analyzed by the 3-(4,5-dimethylthiazol-2-yl)-2,5-diphenyltetrazolium bromide assay. *, $P < 0.05$ compared with A549/Mock (ANOVA). *C,* the invasion activity was measured by the percentage of cells migrated through Matrigel-coated filters in transwell chambers. *, $P < 0.05$, compared with A549/Mock cells. #, $P < 0.05$, compared with A549/ICAM-1. *D,* the inhibitory effect of thalidomide on A549/ICAM-1 – induced cell invasion. *, $P < 0.05$, compared with basal. *E,* top, A549/Mock or A549/ICAM-1 cells were i.v. injected into the lateral tail vein of nude mice, and anti-ICAM-1 antibody was also i.v. injected as described in Materials and Methods. Animals were killed 2 weeks after injection, and lungs were excised and photographed (*white arrows,* metastatic tumor nodules). Bottom, quantitative data of metastatic tumor nodules in different groups. *, $P < 0.05$, compared with A549/Mock. #, $P < 0.05$, compared with A549/Mock or A549/ICAM-1. *F,* top, A549/Mock or A549/ICAM-1 cells were i.v. injected into the lateral tail vein of nude mice and one group of mice were orally treated with thalidomide (*Thali*) as described in Materials and Methods. Animals were killed 2 weeks after injection, and lungs were excised and photographed (*white arrows,* metastatic tumor nodules). Bottom, quantitative data of metastatic tumor nodules in different groups. *, $P < 0.05$, compared with A549/Mock. #, $P < 0.05$, compared with A549/ICAM-1.

To evaluate the inhibition of thalidomide on angiogenesis and tumor formation, the expression of vascular endothelial growth factor and ICAM-1 protein in the excised tumors was examined by Western blotting. As shown in Fig. 6E, the expression of vascular endothelial growth factor and ICAM-1 was elevated in excised tumors and was abolished after thalidomide treatment, further demonstrating the involvement of ICAM-1 in carcinogenesis.

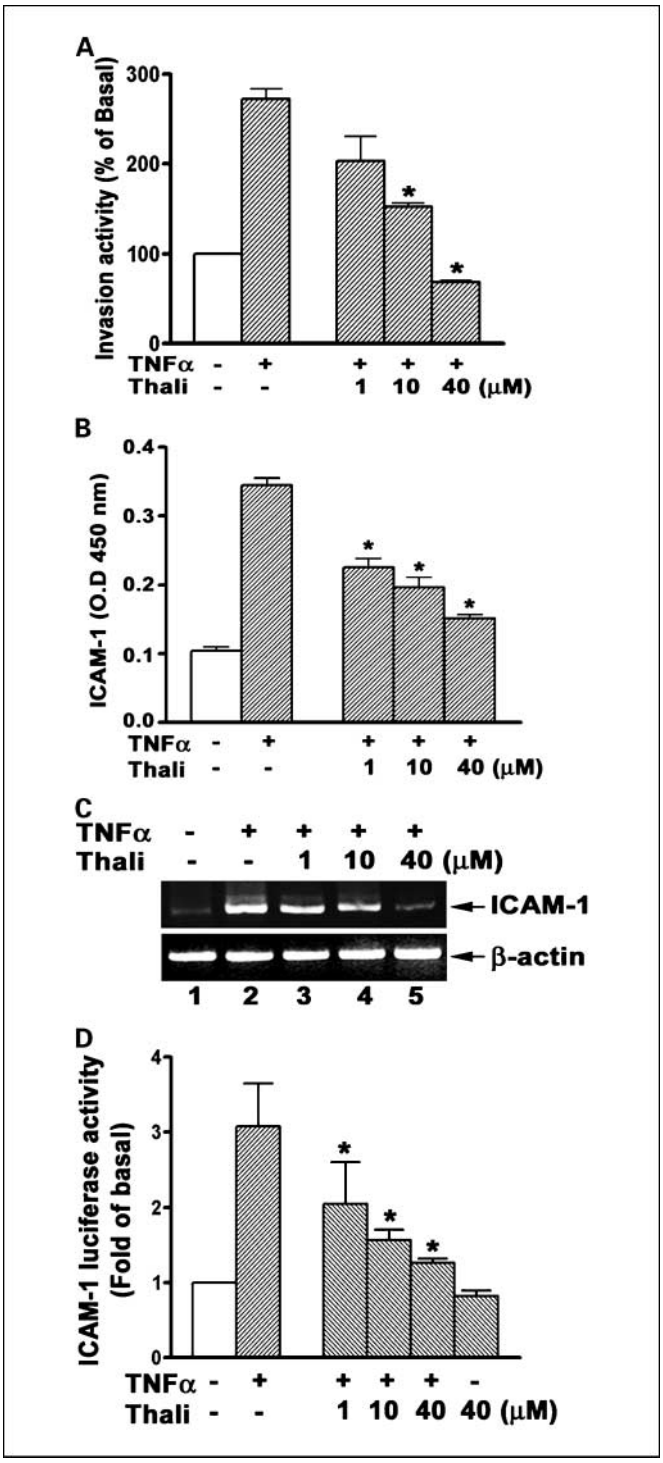

Fig. 3. Inhibitory effect of thalidomide on TNF-α–induced ICAM-1 expression. *A,* the invasion activity of TNF-α–induced A549 cells and the dose-dependent inhibitory effect of thalidomide. *, $P < 0.05$, compared with TNF-α alone. *B,* cells were pretreated with 1 to 40 μmol/L thalidomide for 30 minutes before incubation with 10 ng/mL TNF-α for 4.5 hours. Surface expression of ICAM-1 was measured by ELISA using an anti-ICAM-1 antibody. *, $P < 0.05$, compared with TNF-α alone. *C,* cells were pretreated with 1 to 40 μmol/L thalidomide for 30 minutes before incubation with 10 ng/mL TNF-α for 1 hour. Total RNAs were extracted, and the expression of mRNAs for ICAM-1 and β-actin was analyzed by reverse transcription-PCR. *D,* cells were transfected with pIC339 ICAM-1-luciferase expression vector and then pretreated with 1 to 40 μmol/L thalidomide for 30 minutes before incubation with 10 ng/mL TNF-α for 5 hours. Luciferase activity was normalized with β-galatosidase activity. *, $P < 0.05$ compared with TNF-α alone.

Discussion

Non–small cell lung cancer is the most prevalent type of lung cancer. Although cisplatin-based chemotherapy has been extensively used for the past two decades to treat advanced non–small cell lung cancer, the survival rate is still poor (22). Thus, the search of a new target is important for lung cancer therapy. We showed that ICAM-1 is a molecular target for lung cancer. It promotes cancer formation and metastasis, and thalidomide can effectively inhibit these events through suppression of NF-κB activation.

ICAM-1 is up-regulated in response to a variety of cytokines and is associated with inflammatory and immune responses

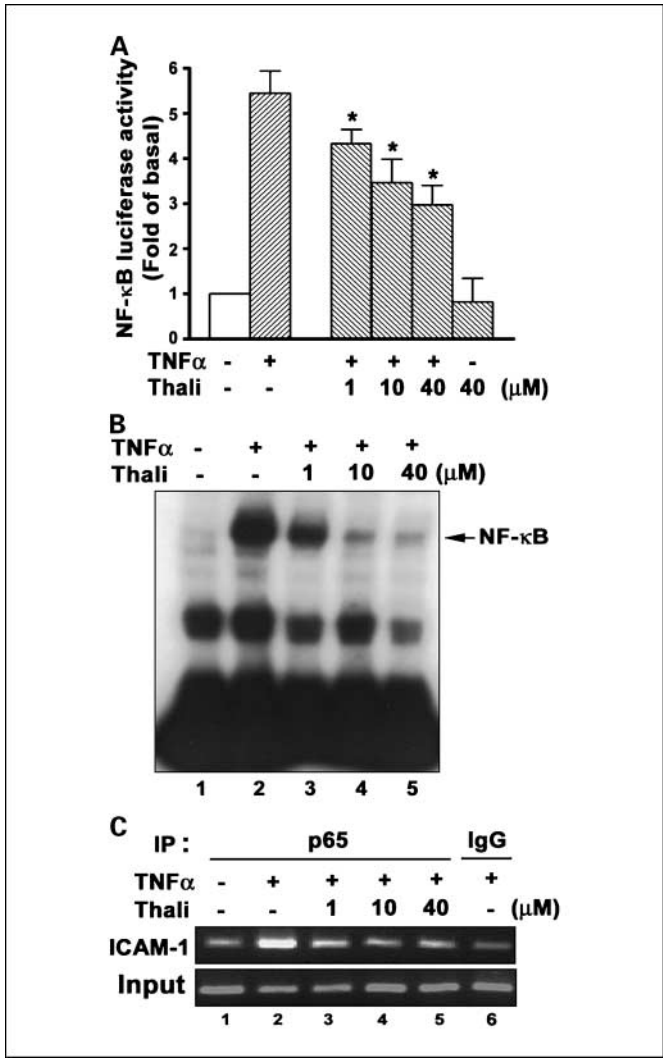

Fig. 4. Inhibitory effect of thalidomide on TNF-α–induced NF-κB activity in A549 cells. *A,* cells were transfected with the NF-κB-luciferase and β-galatosidase vectors, then pretreated with 1 to 40 μmol/L thalidomide for 30 minutes before incubation with 10 ng/mL TNF-α for 5 hours. Luciferase activity was normalized with β-galatosidase activity. *, $P < 0.05$, compared with TNF-α alone. *B,* cells were pretreated with 1 to 40 μmol/L thalidomide for 30 minutes before incubation with 10 ng/mL TNF-α for 60 minutes. κB-binding activity was detected by incubating nuclear extracts (10 μg) with ^{32}P-labeled double-stranded κB oligonucleotide corresponding to the *ICAM-1* gene. *C,* cells were pretreated with 1 to 40 μmol/L thalidomide for 30 minutes before incubation with 10 ng/mL TNF-α for 60 minutes. The binding of p65 to the ICAM-1 promoter was examined by chromatin immunoprecipitation (*IP*) assay. Relevant ICAM-1 promoter sequences were amplified by PCR from complexes immunoprecipitated by anti-p65 antibody.

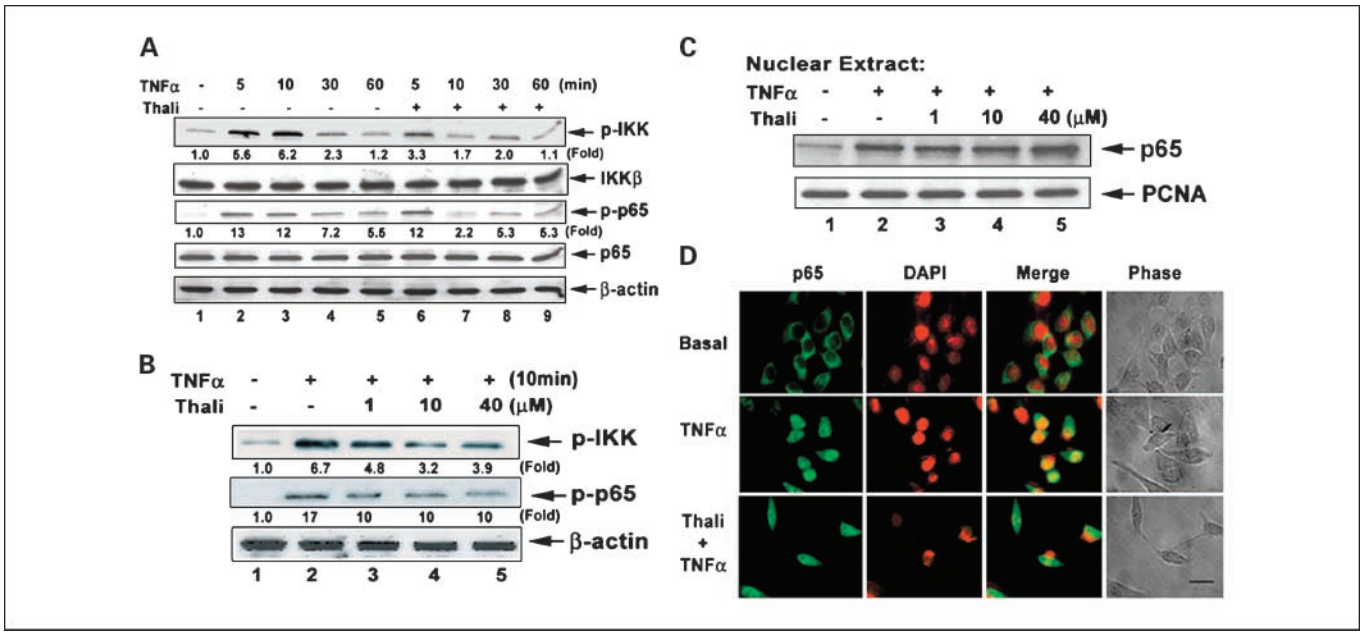

Fig. 5. Effect of thalidomide on TNF-α–induced phosphorylation of IKK and p65 in A549 cells. *A,* cells were pretreated with 10 μmol/L thalidomide for 30 minutes before incubation with 10 ng/mL TNF-α for the indicated time. *B,* cells were pretreated with 1 to 40 μmol/L thalidomide for 30 minutes before incubation with 10 ng/mL TNF-α for 10 minutes. Whole-cell lysates were immunoblotted using anti-phospho-IKK, anti-IKKβ, anti-phospho-p65, anti-p65, or anti-β-actin antibody. *C,* cells were pretreated with 1 to 40 μmol/L thalidomide for 30 minutes before incubation with 10 ng/mL TNF-α for 60 minutes. Nuclear extracts were analyzed by anti-p65 or an anti–proliferating cell nuclear antigen (*PCNA*) antibody. *D,* cells were pretreated with 1 μmol/L thalidomide for 30 minutes before incubation with 10 ng/mL TNF-α for 60 minutes. The cellular localization of p65 was examined by anti-p65 antibody (*green*). 4′,6-Diamidino-2-phenylindole (*DAPI, red*) is a marker for nuclei. 4′,6-Diamidino-2-phenylindole staining was falsely colored red for easier visualization of the merge (overlay). TNF-α–induced translocation of p65 to the nuclei was indicated by colocalization with 4′,6-diamidino-2-phenylindole (*yellow staining in overlay*). Representative morphology of A549 cells was photographed (*gray phase*).

(23). In addition to its role in leukocyte adhesion and cancer cell invasion (9, 12), several lines of evidence in this study show that ICAM-1 plays an important role in tumorigenesis and metastasis. First, ICAM-1 protein expression was higher in the specimens with advanced lung cancer, especially those in stages III and IV. Second, tumors excised from nude mice s.c. injected with A549 lung cancer cells showed high expression of ICAM-1. Third, i.v. injection of A549/ICAM-1 cells into the nude mice induced more metastatic lung nodules than A549/Mock cells. Fourth, A549/ICAM-1 cells induced more invasion than A549/Mock. Cell invasion and tumor metastasis induced by A549/ICAM-1 cells were inhibited by the specific anti-ICAM-1 antibody. However, the inhibition of the *in vitro* cell invasion was greater than that of the *in vivo* metastasis. It is probable that more factors, such as stability and distribution, might be involved in the effect of the *in vivo* application of anti-ICAM-1 antibody. Although ICAM-1 has been reported to be associated with myeloma and breast cancer cell invasion, we provide the direct evidence that ICAM-1 is required for lung cancer formation and metastasis. Adhesion molecules expressed in cancer cells can attract inflammatory cells such as macrophages or lymphocytes, which release trophic factors to enhance cancer cell survival and facilitate instability of tumor environment (24, 25). For example, tumor-associated macrophage, the major component of the infiltrating inflammatory cells, had been reported to release growth and angiogenic factors that stimulate tumor cell proliferation, promote angiogenesis, and even favor invasion and metastasis (26, 27). In this study, human lung cancer with higher ICAM-1 expression aggregated more leukocytes and macrophages,[4] suggesting the dependence on ICAM-1 for the recruitment of inflammatory cells by tumor cells. This ICAM-1–mediated leukocyte accumulation may be a potential trigger for tumorigenesis.

Cancer cells use adhesion mechanisms to aid its migration and homing to distant metastatic sites (25). A549 cells overexpressing ICAM-1 were established to show the direct role of ICAM-1 in the *in vitro* cell invasion and *in vivo* tumor metastasis. These results were further strengthened by the clinical characteristics of human lung carcinoma—high ICAM-1 expression was associated with more metastatic nodules, lymph node metastasis, and poor differentiation (Table 1). According to the logic regression model to analyze multiple outcomes in 40 lung adenocarcinoma patients, ICAM-1 might indirectly affect tumor status and could predict lung cancer patients' tumor status and prognosis. Hence, ICAM-1 might be a potential marker for the evaluation of the outcome of lung cancer patients. Metastasis is a highly organized process (28). The first phase consists of changes in tumor cell adhesion, induction of cell motility, and invasion to local sites, followed by dissemination to regional lymph nodes or circulation and homing to secondary organs (29, 30). Some metastatic cells may eventually become precursors of secondary tumors that arise years after resection of the primary tumor (31). In the present study, we first showed that *in vivo* metastasis was induced by ICAM-1–overexpressing A549 cells. ICAM-1 can be

[4] Unpublished observation.

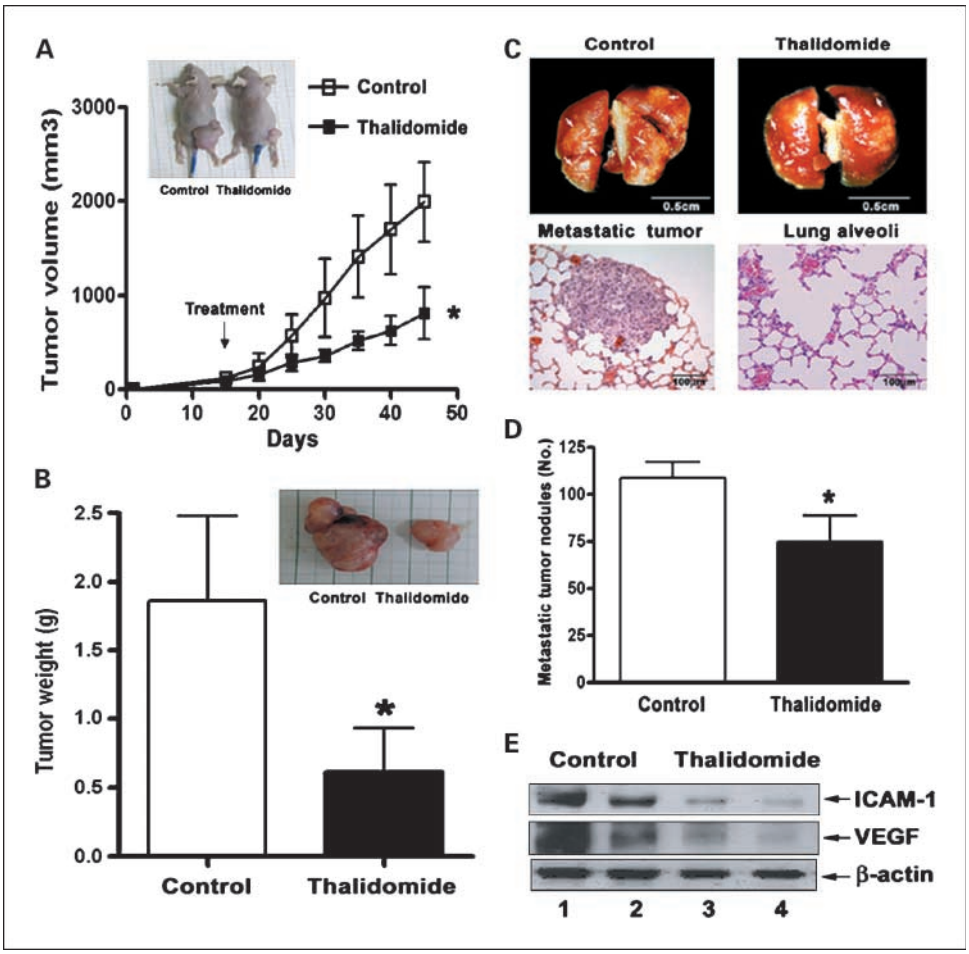

Fig. 6. *In vivo* effect of thalidomide on xenograft tumor growth and metastasis. *A,* A549 cells (10^7) were xenotransplanted into the right hip region of nude mice. After visible tumor formation, mice were randomly divided into two groups for oral treatment with thalidomide or vehicle as described in Materials and Methods. The tumor volume was calculated as follows: $V = 0.52 \times$ (the length of width)$^2 \times$ (the length of length). *, $P < 0.05$, compared with control (ANOVA). *B,* tumors were dissected and weighed. Photographs, tumors from vehicle-treated and thalidomide-treated mice. *, $P < 0.05$ compared with control. *C,* top, lungs were excised and photographed (*white arrows,* metastatic tumor nodules). Bottom, histologic analysis of lung metastasis of vehicle- and thalidomide-treated mice. Left, a metastatic tumor within the lung parenchyma of vehicle-treated mice. Right, thalidomide-treated mice with fewer metastatic tumors and more normal lung alveoli. *D,* the metastatic nodules of vehicle- and thalidomide-treated mice were counted. *, $P < 0.05$, compared with control. *E,* protein lysates obtained from two randomly selected xenograft tumors were electrophoresed and immunoblotted with anti-ICAM-1, anti – vascular endothelial growth factor (*VEGF*), or anti-β-actin antibody.

an important target for metastasis and might develop as a new biomarker for metastatic lung cancer. The mechanism of ICAM-1 – mediated metastasis was probably linked to its outside-in signaling. It has been shown that ICAM-1 can initiate a calcium-mediated signal in breast cancer cells (32). ICAM-1 engagement has also been documented to activate the oncogenic mitogen-activated protein kinase/extracellular signal-regulated kinase cascade through phosphorylation, resulting in activator protein-1 activation and production of cytokine, such as interleukin-8 and RANTES; adhesion molecules (ICAM-1 and vascular cell adhesion molecule-1); matrix metalloproteases; and reactive oxygen species (33 – 36).

Thalidomide has been shown to be a first-line or salvage therapy in patients with multiple myeloma (16). Chemotherapy (cisplatin, cyclophosphamide, epirubicin, and etoposide) with or without thalidomide for lung cancer on clinical trails has been reported (37). Our study on preclinical trial addresses the efficiency of thalidomide in lung adenocarcinoma, a subtype of non – small cell lung cancer. Several studies have reported that thalidomide reduces vascular endothelial growth factor expression in tumor tissues, leading to a dramatic decrease in vascular density and permeability, and an increase in tumor cell apoptosis (38). Our results also showed that thalidomide inhibits the overexpression of vascular endothelial growth factor in tumors excised from nude mice. However, two lines of evidence showed that the anticancer effect of thalidomide was associated with the inhibition of ICAM-1. First, A549/ICAM-1 – induced *in vitro* cell invasion and *in vivo* metastasis were inhibited by thalidomide. Second, high expression of ICAM-1 in tumors excised from nude mice s.c. injected with A549 cells disappeared when treated with thalidomide. To our knowledge, this is the first report linking thalidomide and ICAM-1 in tumorigenesis. The inhibition of tumor growth and metastasis by thalidomide in a preclinical lung cancer xenograft model supports the finding that thalidomide may be a potential chemotherapeutic agent for lung cancer. NF-κB is crucial for TNF-α – induced ICAM-1 expression (13). Thalidomide was shown to attenuate the phosphorylation of IKK and p65, and to inhibit the binding of NF-κB to the ICAM-1 promoter. CYL-19s and CYL-26z, two structurally related α-methylene-γ-lactone compounds, were also identified by this laboratory to show inhibition of TNF-α – induced ICAM-1 expression and ICAM-1 – elicited cell invasion (9). Their mechanism of action was shown to be inhibition of the TNF-α – induced IκBα phosphorylation and degradation, and NF-κB activation via direct targeting of the IKK complex. Although both thalidomide and α-methylene-γ-lactone compounds have inhibitory effect on NF-κB activation and ICAM-1 expression, their chemical structures are different. Moreover, α-methylene-γ-lactone compounds are IKK inhibitors that inhibit IκBα degradation (9); however, thalidomide did not inhibit IκBα degradation (data not shown) and p65 translocation (Fig. 5C and D).

In summary, ICAM-1 is a molecular target for lung cancer. Its role in tumorigenesis, including cancer formation and metastasis, was shown. New insight on how thalidomide suppression of ICAM-1–dependent metastasis and of NF-κB activation is effective in cancer therapy was also shown. ICAM-1 might be developed as new biological marker for the diagnosis of lung cancer. These studies provide a framework for targeting ICAM-1 as a biologically based therapy for cancer.

References

1. DeCicco KL, Tanaka T, Andreola F, De Luca LM. The effect of thalidomide on non-small cell lung cancer (NSCLC) cell lines: possible involvement in the PPARγ pathway. Carcinogenesis 2004;25:1805–12.
2. Manegold C. Chemotherapy for advanced non-small cell lung cancer: standards. Lung Cancer 2001;34: S165–70.
3. Chun KH, Kosmeder JW, Sun S, et al. Effects of deguelin on the phosphatidylinositol 3-kinase/Akt pathway and apoptosis in premalignant human bronchial epithelial cells. J Natl Cancer Inst 2003;95:291–302.
4. Johnson JP. Cell adhesion molecules in the development and progression of malignant melanoma. Cancer Metastasis Rev 1999;18:345–57.
5. Springer TA. Adhesion receptors of the immune system. Nature 1990;346:425–34.
6. Springer TA, Dustin ML, Kishimoto TK, Marlin SD. The lymphocyte function-associated LFA-1, CD2, and LFA-3 molecules: cell adhesion receptors of the immune system. Annu Rev Immunol 1987;5:223–52.
7. Greenwood J, Amos CL, Walters CE, et al. Intracellular domain of brain endothelial intercellular adhesion molecule-1 is essential for T lymphocyte-mediated signaling and migration. J Immunol 2003;171:2099–108.
8. Duperray A, Languino LR, Plescia J, et al. Molecular identification of a novel fibrinogen binding site on the first domain of ICAM-1 regulating leukocyte-endothelium bridging. J Biol Chem 1997;272:435–41.
9. Huang WC, Chan ST, Yang TL, Tzeng CC, Chen CC. Inhibition of ICAM-1 gene expression, monocyte adhesion and cancer cell invasion by targeting IKK complex: molecular and functional study of novel α-methylene-γ-butyrolactone derivatives. Carcinogenesis 2004;25:1925–34.
10. Rosette C, Roth RB, Oeth P, et al. Role of ICAM1 in invasion of human breast cancer cells. Carcinogenesis 2005;26:943–50.
11. Natali PG, Hamby CV, Felding-Habermann B, et al. Clinical significance of $\alpha(v)\beta_3$ integrin and intercellular adhesion molecule-1 expression in cutaneous malignant melanoma lesions. Cancer Res 1997;57: 1554–60.
12. Chang YJ, Holtzman MJ, Chen CC. Interferon-γ-induced epithelial ICAM-1 expression and monocyte adhesion. Involvement of protein kinase C-dependent c-Src tyrosine kinase activation pathway. J Biol Chem 2002;277:7118–26.
13. Chen C, Chou Y, Sun T, Huang C. Tumor necrosis factor α-induced activation of downstream NF-κB site of the promoter mediates epithelial ICAM-1 expression and monocyte adhesion. Involvement of PKCα, tyrosine kinase, and IKK2, but not MAPKs, pathway. Cell Signal 2001;13:543–53.
14. Chen CC, Chen JJ, Chou CY. Protein kinase cα but not p44/42 mitogen-activated protein kinase, p38, or c-Jun NH(2)-terminal kinase is required for intercellular adhesion molecule-1 expression mediated by interleukin-1β: involvement of sequential activation of tyrosine kinase, nuclear factor-κB-inducing kinase, and IκB kinase 2. Mol Pharmacol 2000;58:1479–89.
15. Voraberger G, Schafer R, Stratowa C. Cloning of the human gene for intercellular adhesion molecule 1 and analysis of its 5′-regulatory region. Induction by cytokines and phorbol ester. J Immunol 1991;147: 2777–86.
16. Franks ME, Macpherson GR, Figg WD. Thalidomide. Lancet 2004;363:1802–11.
17. Eisen T, Boshoff C, Mak I, et al. Continuous low dose thalidomide: a phase II study in advanced melanoma, renal cell, ovarian and breast cancer. Br J Cancer 2000;82:812–7.
18. Stebbing J, Benson C, Eisen T, et al. The treatment of advanced renal cell cancer with high-dose oral thalidomide. Br J Cancer 2001;85:953–8.
19. Singhal S, Mehta J, Desikan R, et al. Antitumor activity of thalidomide in refractory multiple myeloma. N Engl J Med 1999;341:1565–71.
20. Chen CC, Chow MP, Huang WC, Lin YC, Chang YJ. Flavonoids inhibit tumor necrosis factor-α-induced up-regulation of intercellular adhesion molecule-1 (ICAM-1) in respiratory epithelial cells through activator protein-1 and nuclear factor-κB: structure-activity relationships. Mol Pharmacol 2004;66:683–93.
21. Huang WC, Chen CC. Akt phosphorylation of p300 at Ser-1834 is essential for its histone acetyltransferase and transcriptional activity. Mol Cell Biol 2005; 25:6592–602.
22. Hotta K, Kiura K, Ueoka H, et al. Effect of gefitinib ("Iressa," ZD1839) on brain metastases in patients with advanced non-small-cell lung cancer. Lung Cancer 2004;46:255–61.
23. Robert C, Kupper TS. Inflammatory skin diseases, T cells, and immune surveillance. N Engl J Med 1999; 341:1817–28.
24. Aeed PA, Nakajima M, Welch DR. The role of polymorphonuclear leukocytes (PMN) on the growth and metastatic potential of 13762NF mammary adenocarcinoma cells. Int J Cancer 1988;42:748–59.
25. Coussens LM, Werb Z. Inflammation and cancer. Nature 2002;420:860–7.
26. Mantovani A, Bottazzi B, Colotta F, Sozzani S, Ruco L. The origin and function of tumor-associated macrophages. Immunol Today 1992;13:265–70.
27. Mantovani A, Bussolino F, Dejana E. Cytokine regulation of endothelial cell function. FASEB J 1992;6: 2591–9.
28. Fidler IJ. The pathogenesis of cancer metastasis: the "seed and soil" hypothesis revisited. Nat Rev Cancer 2003;3:453–8.
29. Birchmeier C, Birchmeier W, Gherardi E, Vande Woude GF. Met, metastasis, motility and more. Nat Rev Mol Cell Biol 2003;4:915–25.
30. Uhr JW, Scheuermann RH, Street NE, Vitetta ES. Cancer dormancy: opportunities for new therapeutic approaches. Nat Med 1997;3:505–9.
31. Pantel K, Brakenhoff RH. Dissecting the metastatic cascade. Nat Rev Cancer 2004;4:448–56.
32. Rahn JJ, Shen Q, Mah BK, Hugh JC. MUC1 initiates a calcium signal after ligation by intercellular adhesion molecule-1. J Biol Chem 2004;279:29386–90.
33. Hubbard AK, Rothlein R. Intercellular adhesion molecule-1 (ICAM-1) expression and cell signaling cascades. Free Radic Biol Med 2000;28:1379–86.
34. Sano H, Nakagawa N, Chiba R, Kurasawa K, Saito Y, Iwamoto I. Cross-linking of intercellular adhesion molecule-1 induces interleukin-8 and RANTES production through the activation of MAP kinases in human vascular endothelial cells. Biochem Biophys Res Commun 1998;250:694–8.
35. Lawson C, Ainsworth M, Yacoub M, Rose M. Ligation of ICAM-1 on endothelial cells leads to expression of VCAM-1 via a nuclear factor-κB-independent mechanism. J Immunol 1999;162:2990–6.
36. Koyama Y, Tanaka Y, Saito K, et al. Cross-linking of intercellular adhesion molecule 1 (CD54) induces AP-1 activation and IL-1β transcription. J Immunol 1996;157:5097–103.
37. Sridhar SS, Shepherd FA. Targeting angiogenesis: a review of angiogenesis inhibitors in the treatment of lung cancer. Lung Cancer 2003;42:S81–91.
38. Verheul HM, Panigrahy D, Yuan J, D'Amato RJ. Combination oral antiangiogenic therapy with thalidomide and sulindac inhibits tumour growth in rabbits. Br J Cancer 1999;79:114–8.